Fossil systems in the 400d cluster catalog

Voevodkin, Alexey; Borozdin, Konstantin; Heitmann, Katrin; Habib, Salman; Vikhlinin, Alexey; Mescheryakov, Alexander; Hornstrup, Allan; Burenin, Rodion

Published in:
Astrophysical Journal

Link to article, DOI:
10.1088/0004-637X/708/2/1376

Publication date:
2010

Document Version
Publisher's PDF, also known as Version of record

The Astrophysical Journal, 708:1376–1387, 2010 January 10 doi:10.1088/0004-637X/708/2/1376

FOSSIL SYSTEMS IN THE 400d CLUSTER CATALOG

Alexey Voevodkin[1,2], Konstantin Borozdin[1], Katrin Heitmann[1], Salman Habib[1], Alexey Vikhlinin[2,3], Alexander Mescheryakov[2,3], Allan Hornstrup[4], and Rodion Burenin[2]
[1] Los Alamos National Laboratory, Los Alamos, NM 87545, USA
[2] Space Research Institute (IKI), Profsoyuznaya 84/32, Moscow, Russia
[3] Harvard-Smithsonian Center for Astrophysics, 60 Garden Street, Cambridge, MA 02138, USA
[4] National Space Institute, Technical University of Denmark, Juliane Maries Vej 30, 2100 Copenhagen 0, Denmark
Received 2009 January 18; accepted 2009 November 18; published 2009 December 22

ABSTRACT

We report the discovery of seven new fossil systems in the 400d cluster survey. Our search targets nearby, $z \leqslant 0.2$, and X-ray bright, $L_X \geqslant 10^{43}$ erg s^{-1}, clusters of galaxies. Where available, we measure the optical luminosities from Sloan Digital Sky Survey images, thereby obtaining uniform sets of both X-ray and optical data. Our selection criteria identify 12 fossil systems, out of which five are known from previous studies. While in general agreement with earlier results, our larger sample size allows us to put tighter constraints on the number density of fossil clusters. It has been previously reported that fossil groups are more X-ray bright than other X-ray groups of galaxies for the same optical luminosity. We find, however, that the X-ray brightness of massive fossil systems is consistent with that of the general population of galaxy clusters and follows the same L_X–$L_{\rm opt}$ scaling relation.

Key words: catalogs – galaxies: clusters: general – X-rays: galaxies: clusters

Online-only material: color figures

1. INTRODUCTION

Studies of clusters and groups of galaxies have revealed an interesting class of objects—relaxed, X-ray bright systems, dominated in the optical by a giant elliptical galaxy at the center. These systems are usually called "fossil groups" (Ponman et al. 1994), or, if massive enough, "fossil clusters" (Cypriano et al. 2006). The interesting properties of these systems are attributed to their dynamical history, including a lack of mergers for a long time prior to observation, out to $z \leqslant 1$ (as it is shown in simulations; e.g., D'Onghia et al. 2005). Because of their quiescent state, fossil groups and clusters (hereafter FGs) are "frozen in time" as compared to other systems. In X-ray observations FGs appear relaxed, without any obvious sign of recent merging processes. Therefore, FGs provide an opportunity to study a class of objects in which internal structure has not been affected by recent major mergers, i.e., objects characterized primarily by passive evolution.

The number of known FGs is very small, and only a handful of them have been studied in some detail. Before definitive statements can be made for FGs as a well-defined class of objects, the statistics must be improved significantly. Known FGs are massive systems with masses in the range typical for rich groups or for poor clusters of galaxies and they share such scaling relations as X-ray luminosity (L_X)–gas temperature (T), total mass (M)–T, gas entropy$-T$, L_X–galaxies velocity dispersion (σ), optical luminosity ($L_{\rm opt}$)–σ, $\sigma - T$, gas fraction ($f_{\rm gas}$)–T with other groups and clusters (Khosroshahi et al. 2007; Sun et al. 2008). However, FGs are more X-ray bright for the given optical luminosity than normal groups of galaxies (Jones et al. 2003, hereafter J03; Khosroshahi et al. 2007, hereafter K07). The merger histories underlying the origin of the central galaxies in FGs continues to be discussed in the literature; originally, they were thought to be possible endpoints of compact group evolution as driven by dynamical friction (see e.g., Ponman et al. 1994, J03). The masses (and M/L ratio) of fossil systems are generally too large to be explained by this particular mechanism, but the basic merger interpretation remains viable, as has been borne out by recent N-body simulations and semi-analytic calculations. (The precise number of fossil groups predicted is still uncertain, however; we will return to this issue below.) An alternative explanation for fossil group formation is that such systems are "failed" groups which suffer from a lack of L_* galaxies as an accident of birth (Mulchaey & Zabludoff 1999).

The definition of fossil groups and clusters remains somewhat ambiguous, as different researchers use variable criteria to identify these systems. Additionally, systems of a possibly "fossil" nature have been called overluminous elliptical galaxies (OLEGs; Vikhlinin et al. 1999), or isolated overluminous elliptical galaxies (IOLEGs; Yoshioka et al. 2004). Even if the nomenclature differs, all these objects are in essence gravitationally bound groups or clusters of galaxies, with the optical light of the central elliptical galaxy dominating that of all other galaxies in the system.

In this work, we loosely follow the definition of FGs as given in J03, namely, a fossil group is an extended X-ray bright object ($L_{X,\rm Bol} \geqslant 0.25 \times 10^{42}\, h^{-2}$ erg s^{-1}), with $\Delta m_{12} \geqslant 2$ for galaxies lying inside half of the virial radius, where Δm_{12} is the absolute magnitude difference in the R filter between the first and second brightest galaxy. This definition is phenomenological, and it was applied by J03 to identify five such objects. One obvious deficiency of this definition is that it imposes an artificially sharp Δm_{12} threshold (representing the tail of the Schechter function), whereas no such sharp boundary can be found in the Δm_{12} distribution in clusters (Milosavljević et al. 2006; La Barbera et al. 2008). Therefore, for any chosen threshold of Δm_{12} there will always be systems very close to the boundary, and their identification would depend on the accuracy of photometric measurements in optical observations. There is a very similar, but perhaps even more difficult, problem associated with the definition of the radius inside which the second brightest galaxy should be considered. (Figure 1 provides an example of this.) In practice, some researchers use a fixed fraction of the virial

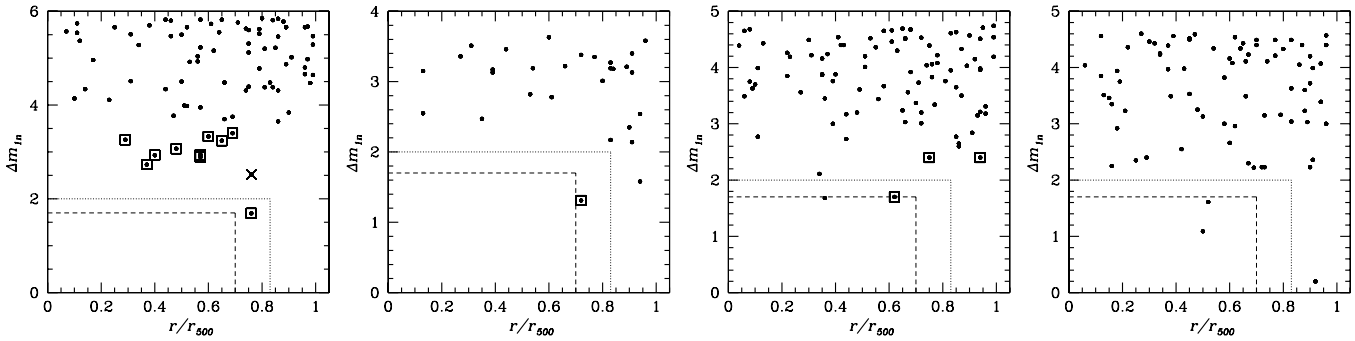

Figure 1. Difference in magnitude Δm_{1n} between the central galaxy of the cluster and other individual galaxies, as a function of distance to the X-ray center. The four panels correspond to clusters (from left to right) cl1159p5531, cl1340p4017, cl1416p2315, and cl1552p2013, identified earlier as fossil systems. Squares denote galaxies with SDSS spectroscopic redshift and $|z_{\rm cluster} - z_{\rm galaxy}| \leqslant 0.005$, and crosses denote galaxies with $|z_{\rm cluster} - z_{\rm galaxy}| > 0.005$. Dotted lines show the Jones criteria for fossil group selection (see the text). We note that none of these four previously known FGs can be identified as fossils, if the strict Jones criteria are accepted (in all cases there are some galaxies inside the solid boxes, implying that $\Delta m_{12} < 2$ within half of the virial radius). Dashed lines show the somewhat more relaxed criteria used in this paper, which maintain the identification of the three previously known FGs as fossil systems.

radius within which the second brightest galaxy is considered, while others look for such a galaxy within some fixed radius (Santos et al. 2007; La Barbera et al. 2008). Finally, the spectroscopic redshift of that second galaxy is often unknown and therefore its group membership cannot be reliably determined. Still, the J03 criteria have the advantage of being definitive and remain the most popular choice for FG identification in observations. We re-evaluate these criteria as part of our analysis below.

In contrast to considering fossil systems as a separate category some researchers speculate that there may be a "fossil phase" in the life of many clusters, with an absence of significant mergers for a long time, enough for cluster relaxation (von Benda-Beckmann et al. 2008). A bright galaxy may subsequently fly into the inner part of the cluster, and the object may now appear to the observer as a normal group or cluster of galaxies.

In order to gain a better understanding of the nature of FGs—as observationally defined—more of these systems have to be observed, and a comparison with normal groups or clusters of galaxies carried out in a uniform manner. We aim here to identify new FGs and to compare their properties with those of other systems in the same mass range.

Our FG search uses the 400d X-ray survey of galaxy clusters (Burenin et al. 2007). The advantage in using X-ray surveys is that in this case our selection is based on the presence of an extended X-ray source, indicating that the object is a gravitationally bound system, and not a chance superposition of galaxies. We can then proceed to identify FGs in the optical band. The 400d survey provides an appropriate database for this work, since almost every cluster has a CCD image in the *R* band. We use different optical data to identify FGs in the 400d survey, but our comparison of FGs with other groups and clusters has been mostly enabled by the Sloan Digital Sky Survey (hereafter SDSS) DR6, providing us with a uniform data set both in the X-ray and in the optical. The survey area as a function of flux is well calibrated, allowing us to put constraints on the FG number density.

In this work, we consider luminous systems with X-ray luminosities $L_X \geqslant 10^{43}$ erg s^{-1}. Masses of these objects, estimated from their X-ray luminosities, correspond to rich groups or poor clusters of galaxies. We generally refer to these systems as clusters to highlight the fact that we study here the bright and massive end of the distribution of fossil systems.

Where we need to assume a cosmology, we choose a ΛCDM model, with $\Omega_M = 0.3$, $\Omega_\Lambda = 0.7$, and $h = 0.71$, the Hubble constant, measured in units of 100 km s^{-1} Mpc^{-1}. X-ray luminosities and fluxes are given in the 0.5–2.0 keV band.

The paper is organized as follows. In Section 2, we describe the available data and the methodology underlying our FG search. In Sections 3–5, we present our results: seven new FGs, constraints on the number density of FGs, and an L_X–L_r correlation. We summarize our findings in Section 6. The Appendix contains a detailed description of all individual fossil systems we study in this paper.

2. DATA ANALYSIS

The 400d cluster survey catalog (Burenin et al. 2007) contains X-ray selected clusters of galaxies from *ROSAT* PSPC high-latitude pointing observations. The area of the sky covered by the survey is 397 deg^2. It includes clusters with fluxes higher than 1.4×10^{-13} erg s^{-1} cm^{-2}—242 clusters in total. Approximately a third of the clusters have redshifts higher than $z = 0.3$, and the catalog may be considered as complete up to $z \approx 1$. Every object has a measured spectroscopic redshift, X-ray flux, and X-ray luminosity. Most of the objects have CCD *R*-band images mainly obtained with the Russian–Turkish 1.5 m telescope in the North and the Danish 1.54 m telescope in the South.[5]

The 160d catalog (Vikhlinin et al. 1998)—a subcatalog of the 400d catalog—was previously used for an FG search (Vikhlinin et al. 1999). In this work, we have decided to use the same selection criteria, i.e., we select clusters with $z \leqslant 0.2$ and $L_X \geqslant 10^{43}$ erg s^{-1}. These cuts provide us with clusters of Abell richness 0 (or higher), being visible on CCD images as galaxy concentrations (see Vikhlinin et al. 1999). Applying these cuts to the complete 400d catalog yields 75 candidates for our FG search.

In the next step, we visually inspect the optical images of the 75 candidates. The purpose of visual inspection is to check the quality of optical images, for instance, bad seeing, low transparency, or existence of a bright star which under long exposures will influence the galactic photometry. It is faster to carry out this procedure manually and it is more reliable than developing algorithms dealing with different effects on images obtained at different telescopes. It turns out that some of candidates do not have optical images of sufficient quality for our purposes. Either the quality of the CCD image does

[5] Some observations were also performed at the Multiple Mirror Telescope, at the ESO 3.6 m, and at the FLWO 1.2 m telescope. Detailed information can be found online at http://hea-www.harvard.edu/400d/catalog/table_cat.html.

not allow for reliable photometry (six images), or the image was originally just a scanned photographic plate (DSS2, nine images). For all bad quality images and eight images with DSS2 data we use archival data from the SDSS DR6 (Adelman-McCarthy et al. 2008). For one cluster with DSS2 data SDSS data are not available, but we find that this cluster is a member of ENACS survey (Katgert et al. 1998) and use information from this survey. After that we decide to use SDSS data whenever possible, because they provide us with photometry of galaxies from sky areas much larger than cluster area. We have SDSS data for 38 clusters from the original sample. For the remaining 37 clusters, we work with good quality *R*-band CCD images.

Below, we use SDSS *r*-filter (model) magnitudes corrected for galactic extinction following Schlegel et al. (1998), and use the program kcorrect version 4.1.4 (Blanton & Roweis 2007) to transform them galaxy luminosities. If SDSS data are not available we make measurements using *R*-band CCD plates.

2.1. Identification of Fossil Groups

In 2003, nine years after the discovery of the first fossil system by Ponman et al. (1994) and several other detections of fossil systems, J03 proposed the first concrete definition of FGs. Since then, this definition has been adopted by most of the community, and new FGs have been detected by various research groups. A major difficulty from the observational perspective is to ensure that all galaxies belonging to the system have been identified. For example, RX J1552.2+2013 was identified (J03) as an FG and later studied again (Mendes de Oliveira et al. 2006) in detail. It was only recently found (Zibetti et al. 2008) that this system does not in fact obey the Jones criteria: a bright galaxy within half of the virial radius had not been seen in previous exposures, which only covered a fraction of the half-virial radius circle around the central galaxy. As another example, the object RX J1159.8+5531 was studied by Vikhlinin et al. (1999) and identified as an OLEG. However, it was found from SDSS data (Diaz-Gimenez et al. 2008) that a bright galaxy inside half of the virial radius had been missed previously, and therefore the system should not have qualified as an FG. We discuss these examples to caution the reader that even if a system has been previously identified as an FG, new studies with better data may reveal that the identification is erroneous.

Another question concerns the accuracy of the photometry obtained for the galaxy members of the system. The standard definition of an FG requires $\Delta m_{12} \geqslant 2$, but depending on the observational conditions and the methods used, the galaxy flux measurements for the same object might differ. We therefore view the optical criteria suggested by J03—$\Delta m_{12} \geqslant 2$ within half the virial radius—as guidelines rather than strict requirements.

As a first check for our sample of 75 FG candidates, and to provide a baseline, we consider the systems previously identified as FGs. Such systems allow us to cross-check our observational results with the analysis carried out by other groups and to re-evaluate the Jones criteria. We find six known FGs present in our sample (see Table 4 in Mendes de Oliveira et al. 2006). They are cl1159p5531, cl1340p4017, cl1416p2315, cl1552p2013, cl2114m6800, and cl2247p0337.[6] The first four of these systems have been observed by the SDSS and therefore uniform measurements are available.

In order to identify a system as an FG, we first have to establish a search radius to identify group members and measure Δm_{1n}. Following the standard definition, the search radius should be some fraction of the virial radius. Using the cluster X-ray luminosities from the 400d catalog we can estimate r_{500} for every cluster in our sample from (Vikhlinin et al. 2008):

$$r_{500} = 8.17\times10^{-7}\left(\frac{L_X}{\mathrm{erg\ s^{-1}}}\right)^{0.21}\left(\frac{h}{0.72}\right)^{-0.59}E(z)^{-1.05}, \quad (1)$$

where $E(z) = \sqrt{\Omega_M(1+z)^3+\Omega_\Lambda}$ (for a flat universe), and r_{500}, measured in kpc, is the radius inside which the mean cluster density is 500 times higher than the critical density of the universe. The radius r_{500} can be determined from Equation (1) with an uncertainty of approximately 8%. The relation between r_{500} and the virial radius is given by $r_{500} \approx 0.6r_{\rm vir}$. Therefore, r_{500} covers a slightly larger area than suggested by the Jones criteria. We decide to keep this more conservative limit for our search radius as a starting point.

Figure 1 shows our results for the four clusters previously identified as fossil systems, using the available SDSS data. We show the dependence of Δm_{1n} on the distance to the X-ray center. The squares around dots indicate galaxies for which spectroscopic redshifts are available and which belong to the group (see the next subsection). It is obvious from all four panels that the central galaxies in these groups are isolated inside some radius, but that the identification of the system as an FG depends critically on the search radius. The groups cl1159p5531 and cl1340p4017 are FGs if the search radius is equal to $0.7r_{500}$ which is slightly smaller than half the virial radius. The group cl1416p2315 is an FG if we relax the $\Delta m_{12} \geqslant 2$ criterion to $\Delta m_{12} \geqslant 1.7$.[7] As for the group cl1552p2013, there are two galaxies within $0.7r_{500}$ and $\Delta m_{1n} < 1.7$. Clearly, this system had been misidentified as an FG previously (this conclusion agrees with a recent analysis by Zibetti et al. 2008).

Based on the first three cases, we adopt a slightly relaxed optical criterion for our sample to identify FGs in comparison to those of J03: we classify an object as an FG if $\Delta m_{12} \geqslant 1.7$ for galaxies inside $0.7r_{500}$. Almost the same criterion, $\Delta m_{12} \geqslant 1.75$, was used by La Barbera et al. (2008), with the aim of optimizing the number of FGs found relative to random coincidences. The search radius we choose is not much different from the assumed search radius of $0.5r_{\rm vir}$. Indeed, $r_{500} \approx 0.6r_{\rm vir}$, and we should take into account that r_{500} found from the L_X–M_{500} correlation has its own uncertainties. The radius $0.7r_{500}$ corresponds to the lowest 2σ boundary of $0.5r_{\rm vir}$.

3. SEARCH FOR NEW FOSSIL GROUPS

After having established criteria for identifying FGs from the three previously known FGs, and setting aside the one previously misidentified, we now analyze the remaining 71(34 of them have SDSS data) clusters in our sample. We divide these clusters into two sub-groups: those for which we have optical data from the SDSS and those for which we have to rely on optical data from other telescopes.

3.1. Clusters with SDSS Data

Working with SDSS data, we select galaxies with good photometry following the recommendations from Oyaizu et al.

[6] Here and below we use object names from the 400d catalog. The meaning of these names is straightforward: the first four digits represent the right ascension, the last four, the declination, p and m denote plus and minus signs for the Northern and Southern hemispheres, respectively.

[7] The galaxy at $0.35r_{500}$ with $\Delta m_{1n} \approx 1.7$, R.A. = $14^{\rm h}16^{\rm m}21\overset{\rm s}{.}8$ and decl. = $+23^\circ17^{\rm m}22\overset{\rm s}{.}8$ does not belong to the group according to its spectroscopic redshift (see Cypriano et al. 2006).

Table 1
FGs Sample

Name	z	Δm_{12}	R.A.[a]	Decl.[a]	Data Type[b]	Notes[c]	Reference
cl0245p0936	0.147	2.15	02:45:48.2	+09:36:21.7	RTT150	New	...
cl0259p0013	0.194	2.25	02:59:33.1	+00:16:25.8	SDSS	New	...
cl0532m4614	0.135	1.90	05:32:40.3	−46:11:54.4	LCO-40	New	...
cl1038p4146	0.125	1.87	10:37:54.8	+41:44:32.1	SDSS	New	...
cl1042m0008	0.138	1.80	10:42:17.4	−00:09:34.7	SDSS	New	...
cl1110m2957	0.200	1.78	11:10:03.3	−29:58:31.1	Danish 1.54 m	New	...
cl1159p5531	0.081	2.73	11:59:34.9	+55:30:39.5	SDSS	FG or OLEG	Vikhlinin et al. (1999)
cl1340p4017	0.171	2.47	13:40:39.3	+40:18:25.6	SDSS	FG or OLEG	Ponman et al. (1994)
cl1416p2315	0.138	1.70	14:16:32.0	+23:19:06.8	SDSS	FG	J03
							Cypriano et al. (2006)
							Khosroshahi et al. (2006)
cl2114m6800	0.130	1.99	21:14:24.0	−68:00:55.5	Danish 1.54 m	OLEG	Vikhlinin et al. (1999)
cl2220m5228	0.102	2.21	22:19:49.0	−52:27:12.9	ENACS	New	...
cl2247p0337	0.200	2.56	22:47:27.9	+03:38:14.5	RTT150	OLEG	Vikhlinin et al. (1999)

Notes.
[a] R.A. and decl. are coordinates of the second brightest galaxy inside our search radius, $0.7r_{500}$.
[b] Data type used.
[c] Whether the object was previously known as an FG or was found in this work.

(2008). We also make use of SDSS spectroscopic redshifts, whenever they are available.

We accept a given galaxy as belonging to the target cluster if $|z_{\rm cluster} - z_{\rm galaxy}| \leqslant 0.005$, where $z_{\rm cluster}$ is the cluster redshift cited in the 400d catalog. The selected threshold for cluster membership, $z = 0.005$, corresponds approximately to a 2σ velocity dispersion (1500 km s^{-1}) for the most massive clusters from our sample. This criterion helps us to remove large foreground spiral galaxies from consideration. If a galaxy inside our search radius does not have a spectroscopic redshift, it is considered as belonging to the cluster.

Applying our FG criteria to clusters with SDSS data we find three new fossil systems: cl0259p0013, cl1038p4146, and cl1042m0008. Some of their properties are listed in Table 1.

3.2. Clusters with Non-SDSS Optical Data

In our sample there are 37 clusters for which we use *R*-band CCD observations. We use the SExtractor program to perform the analysis of the CCD plates. We set the detection threshold equal to 4σ–5σ over the background level and in order to be consistent with SDSS photometry, we measure the galaxy fluxes in Petrosian apertures. The definition of Petrosian aperture used in SExtractor differs from the one used in the SDSS program Photo. Therefore, in Figure 2 we compare the difference in apparent magnitudes between the brightest and all other galaxies, Δm_{1n}, obtained with SExtractor (Bertin & Arnouts 1996) on the corrected frame SDSS image versus SDSS DR6 *r*-filter photometry. The Δm_{1n} for brightest galaxies between outputs is in agreement within 0.1 mag, corresponding to the errors claimed both in Photo (see Figure 6 in Abazajian et al. 2009) and SExtractor (see Figure 4 in Bertin & Arnouts 1996). Larger discrepancies only arise for faint galaxies, which are not important for our study. We note that the SDSS archival measurements are done in the *r* filter, while our own measurements are carried out in the *R* filter. This leads to different apparent magnitudes. Therefore, for four reference objects with SDSS data shown in Figure 1 we transform *r*-filter magnitudes to *R*-filter magnitudes using equations from Fukugita et al. (1996). We obtain that for all galaxies shown

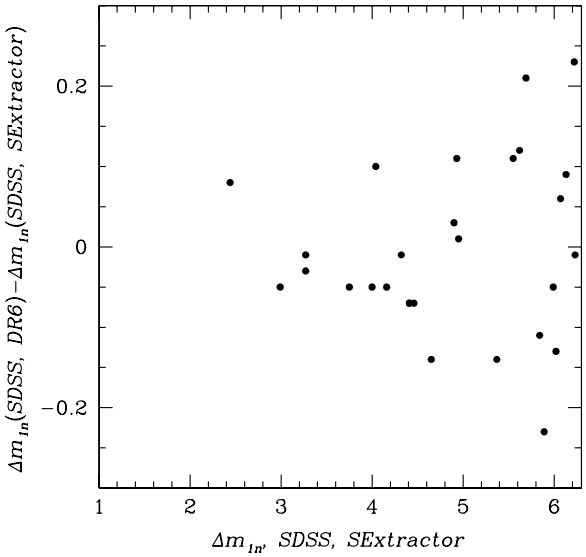

Figure 2. Comparison of the *r*-filter photometry from SDSS DR6 with photometric measurements done by SExtractor on the corrected frame *r*-filter SDSS image for the cluster cl1159p5531.

the quantity Δm_{12} calculated in *R* filter differs less than 0.02 from Δm_{12} calculated in *r* filter. Therefore, FG criterion, $\Delta m_{12} \geqslant 1.7$, formulated using *r* filter magnitudes is also applicable to objects where we can measure Δm_{12} only in *R* filter.

Applying our FG criteria to the data we find an additional set of four new FGs: cl0245p0936, cl0532m4614, cl1110m2957, and cl2220m5228. For the cluster cl2220m5228 we do not have a CCD image from the 400d database, but this cluster is a member of the ENACS survey (Katgert et al. 1998). Using ENACS data we can establish that this cluster is an FG (see the Appendix for details.)

To summarize, we detect seven new FGs in the 400d catalog. Besides cl1552p2013, all previously known FGs satisfy our selection criteria. Table 1 shows the results for all 12 FGs from our sample. In the Appendix, we provide a more detailed description of each system.

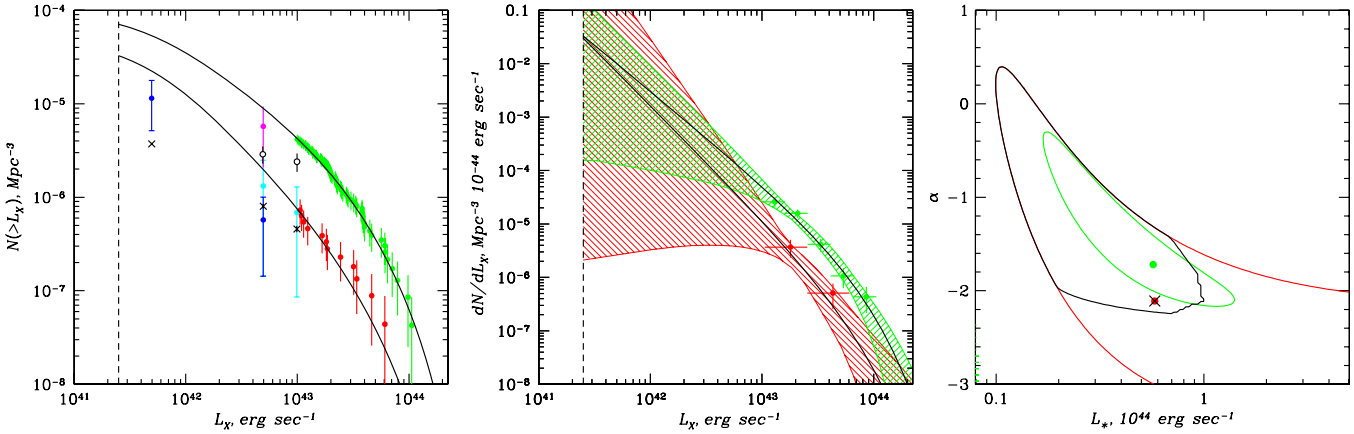

Figure 3. Luminosity functions for fossil systems. Left panel: cumulative luminosity function. Red points correspond to fossil systems and green points correspond to the general population of clusters studied in this work. Black lines are best fits for our data by the Schechter function. Blue, cyan, magenta, and empty black points are previous estimations from J03, Vikhlinin et al. (1998), Romer et al. (2000), and La Barbera et al. (2008), respectively. Black crosses show number densities obtained in simulations (Dariush et al. 2007). Middle panel: differential luminosity functions for FGs (red) and clusters (green) studied in this work. The lines correspond to 1σ sets of the fits obtained with different values of $L_{X,*}$ and α from regions defined by contours on the right panel. Right panel: 1σ confidence contours on parameters of the Schechter function $L_{X,*}$ and α obtained with free normalization. The green contour is for our whole cluster sample, red for FGs, and black for FGs using the constraint that the number density of FGs cannot be greater than the number density of clusters.

(A color version of this figure is available in the online journal.)

4. NUMBER DENSITY OF FOSSIL GROUPS

There are several estimates for the number density of FGs in the literature (Vikhlinin et al. 1998; Romer et al. 2000, J03; Santos et al. 2007; La Barbera et al. 2008). Our sample includes both known and newly identified FGs in the 400d catalog. While our definition for FGs has been derived using only systems for which SDSS data are available, nevertheless it also works well for other previously known FGs without SDSS data: no fossil systems previously detected in the 400d survey were missed. Consequently, we can use our sample to derive a constraint on the number density of FGs as a function of their X-ray luminosity.

In order to find the number density of objects with a given luminosity (luminosity function) we need to know the corresponding survey volume. The 400d survey is a flux limited survey, and therefore we can use standard techniques for the calculation of the volume, where all clusters of a given luminosity would have been detected. The volume is given by (see Burenin et al. 2007 for details)

$$V(L_X) = \int_{0.0032}^{0.20} A(f_X, z)\frac{dV}{dz}dz, \qquad (2)$$

where the lower integration limit corresponds to the 400d cluster with the lowest redshift, the upper integration limit is our limit for sample selection, and the function $A(f_X, z)$ is an effective survey area (see the 400d survey data). We fit our FG sample by a Schechter function(Schechter 1976; the use of the Schechter function is justified below):

$$f(L_X)dL_X = A\left(\frac{L_X}{L_{X,*}}\right)^{\alpha}\exp\left(-\frac{L_X}{L_{X,*}}\right)dL_X, \qquad (3)$$

giving the number of clusters with luminosities from L_X to $L_X + dL_X$ inside a unit volume. We use the maximum likelihood method for unbinned data (Cash 1979), with the best-fit parameters found by maximizing the likelihood function:

$$\ln \pounds = \sum_i \ln(f(L_{X,i})V(L_{X,i})) - \int f(L_X)V(L_X)dL_X. \qquad (4)$$

Table 2
Parameters for the Best-fit Schechter Functions

Sample	A (Mpc^{-3} 10^{-44} erg s^{-1})	$L_{X,*}$ (10^{44} erg s^{-1})	α
FG	$(3.20 \pm 1.61) \times 10^{-7}$	0.58	−2.11
ALL	$(2.87 \pm 0.56) \times 10^{-6}$	0.57	−1.72

Note. Normalization errors are obtained by marginalizing over $L_{X,*}$ and α.

The cumulative luminosity function for our FGs is shown in the left panel of Figure 3 by the red points and the best fit is shown by the black line (the parameters for the fit are given in Table 2).

We also fit the luminosity functions for the entire cluster sample under consideration (75 clusters) via a Schechter function. The results are shown by the green points in the left panel of Figure 3. The best fit is shown by the black line (for the best-fit parameters, see Table 2). In the middle panel of Figure 3 we show the differential luminosity functions for FGs and clusters.

For comparison with previous results we extrapolate the FG and cluster number density fits to $L_X = 2.5 \times 10^{41}$ erg s^{-1} which corresponds to the group boundary (O'Sullivan et al. 2001, J03)—beyond this value objects are more likely to be isolated elliptical galaxies than groups. We use Table 2 from J03 as a compilation of known results. The points from this table, rescaled to the cosmology used here, are shown in the left panel of Figure 3. Blue points correspond to the estimates obtained by J03, cyan corresponds to estimates from Vikhlinin et al. (1999), the magenta point is an estimate from Romer et al. (2000), and the empty black points are estimates from the recent work of La Barbera et al. (2008). The errors on the number densities as found by Romer et al. (2000) and La Barbera et al. (2008) are estimated from Poisson statistics. Black crosses show estimates of FGs number densities obtained in simulations (Dariush et al. 2007).

Overall, our constraints are in good agreement with previous observational results. The FG number density of Romer et al. (2000; magenta point) lies higher than the number densities obtained by others, but their results are based on only three objects and therefore may be considered to be consistent with

the other findings, given the statistical uncertainty. Our results are in good agreement with the number density estimation of J03, and in perfect agreement with the estimate from Vikhlinin et al. (1999). The latter agreement is not surprising since their data set is a subset of ours, and the same methodology was used for survey area calibration. The number density estimation from La Barbera et al. (2008) agrees with the extrapolation of our result, but it is too high for FGs brighter than 10^{43} erg s^{-1}. We note that the search radius, 350 kpc, chosen in that work is smaller than the half-virial radius for such X-ray bright objects, possibly causing an overall overestimation of the FG number density. We find that our estimation of FGs number density is higher than predicted in simulations of Dariush et al. (2007), though still consistent with it after statistical uncertainties are taken into account. Note, FGs selection criteria and the quality of data sets differ from one work to another. Therefore, all current estimates of FGs number densities should be considered as an attempt to estimate number density of objects which are indeed dominated by single elliptical galaxy, but this "domination" depends strongly both on definition used and on the quality of data. For example, if we try to follow precise J03 definition and choose $\Delta m_{12} \geqslant 2$ for galaxies inside $0.5R_{\rm vir} \approx 0.8r_{500}$ as FGs selection criteria then none of FGs from Table 1 survives.

Despite the increased number of FGs in comparison to previous results, our constraints are still not very tight. In the right panel of Figure 3 we show the 1σ confidence contours for α and $L_{X,*}$ obtained with a free normalization parameter (red represents FGs and green, clusters). In the middle panel of Figure 3 we show the sets of fits corresponding to the contours on the right panel via red and green shaded regions. We can reduce the range of allowed values for $L_{X,*}$ and α for the FG fit by taking into account the constraint that the FG number density cannot be higher than the number density of clusters (at least in the luminosity range where the phrase "group of galaxies" is still valid, i.e., where $L_X \geqslant 2.5 \times 10^{41}$ erg s^{-1}). This is done by forcing likelihood function, Equation (4), to be unacceptably small if for the given set of parameters the fit of FGs number density intersects the best fit of clusters number density in the range of luminosities considered here. As a result, the best fit of FGs number density remains the same with and without the constraint, but the 1σ intervals for α and $L_{X,*}$ become tighter (black contour in the right panel of Figure 3).

As can be seen from the left and middle panels of Figure 3, the Schechter function provides a very good fit to the cluster luminosity function. This is not surprising since even a simple theory of large-scale structure formation (Press & Schechter 1974) predicts Schechter-like functions. Since the cluster luminosity is connected with the cluster mass via a power-law relation and the range of luminosities considered here covers only one decade of luminosities, Equation (3) has enough degrees of freedom to fit the mass function or the luminosity function in our case. Our extrapolation beyond the data range should certainly be treated with caution, but we do this mainly to compare our results with previous studies.

We fit the FG luminosity function with a Schechter function as well. The simple justification is that FGs are a subset of the cluster sample, and the shape of their luminosity function should be similar to the shape of the cluster luminosity function. A more precise result for the FG number density may be obtained by using the extended Press–Schechter formalism (Milosavljević et al. 2006), but for a sample of only 12 objects this is hardly necessary.

5. L_X–L_R RELATION

It was shown in J03 and K07 that for a given X-ray luminosity, FGs are less luminous in the optical band as compared to (X-ray bright) normal groups of galaxies. However, these comparisons were not uniform, i.e., the data for FGs and other systems were obtained separately, using different methods of data analysis. In order to avoid these caveats and make uniform measurements of optical luminosities of both FGs and other clusters we use only systems with SDSS data (38 objects). As elsewhere in this paper, we use X-ray luminosities from the 400d catalog.

5.1. Measurements of Optical Luminosities

We use SDSS data to select galaxies around the X-ray centers of the clusters. We select all galaxies brighter than $m^{\rm thresh} = 21$ and require the photometry flags to be the same as in Section 2. The selected threshold is 1.2 mag lower than the threshold in the *r* filter providing 95% SDSS completeness (Adelman-McCarthy et al. 2008). With this threshold, galaxies can be selected based on reliable detection in all filters with small statistical errors. Since the redshifts are known only for a small number of galaxies (0–15), in order to exclude background galaxies from the contribution to cluster luminosity, we carry out the following steps:

1. Exclude central cD galaxies.
2. Mask regions around bright stars and foreground galaxies which angular size more than $0.1r_{500}$ and exclude masked area from further consideration. The bright stars are masked because the photometry of faint galaxies around such stars may be incorrect. We use SDSS photometric flags to identify such galaxies. We also do not consider galaxies with SDSS spectroscopic redshifts if $|z_{\rm cluster} - z_{\rm galaxy}| > 0.005$.
3. Estimate the lost light due to the selected magnitude threshold. We subtract the background luminosity function from the cluster luminosity function, where the cluster luminosity function is built for galaxies around the X-ray center within a radius of $0.5r_{500}$, and a background function is built for galaxies inside the ring with radii from $2r_{500}$ to $3r_{500}$. We fit the residual by a Schechter function written in the form:

$$\phi(m)dm = \phi_0 10^{0.4(m_*-m)(\alpha+1)} \exp(-10^{0.4(m_*-m)})dm. \quad (5)$$

The fraction of the lost light is given by

$$f = \Gamma(\alpha+2, 10^{0.4(m_*-m^{\rm thresh})})/\Gamma(\alpha+2). \quad (6)$$

This fraction varies from object to object, and its values lie in the range from 2% to 30%. The chosen radius, $0.5r_{500}$, represents the most luminous part of the cluster where contribution from background galaxies is negligibly small (less than 5%). The derived corrections are not sensitive to small ($\pm 0.1r_{500}$) variations in its value.
4. Transform magnitudes of all galaxies inside $3r_{500}$ to luminosities with *K*-corrections (kcorrect ver. 4.1.4; Blanton & Roweis 2007) for cluster redshift. Build the light profile by summing luminosities of individual galaxies inside the rings around the cluster center and exclude regions masked in step 2).

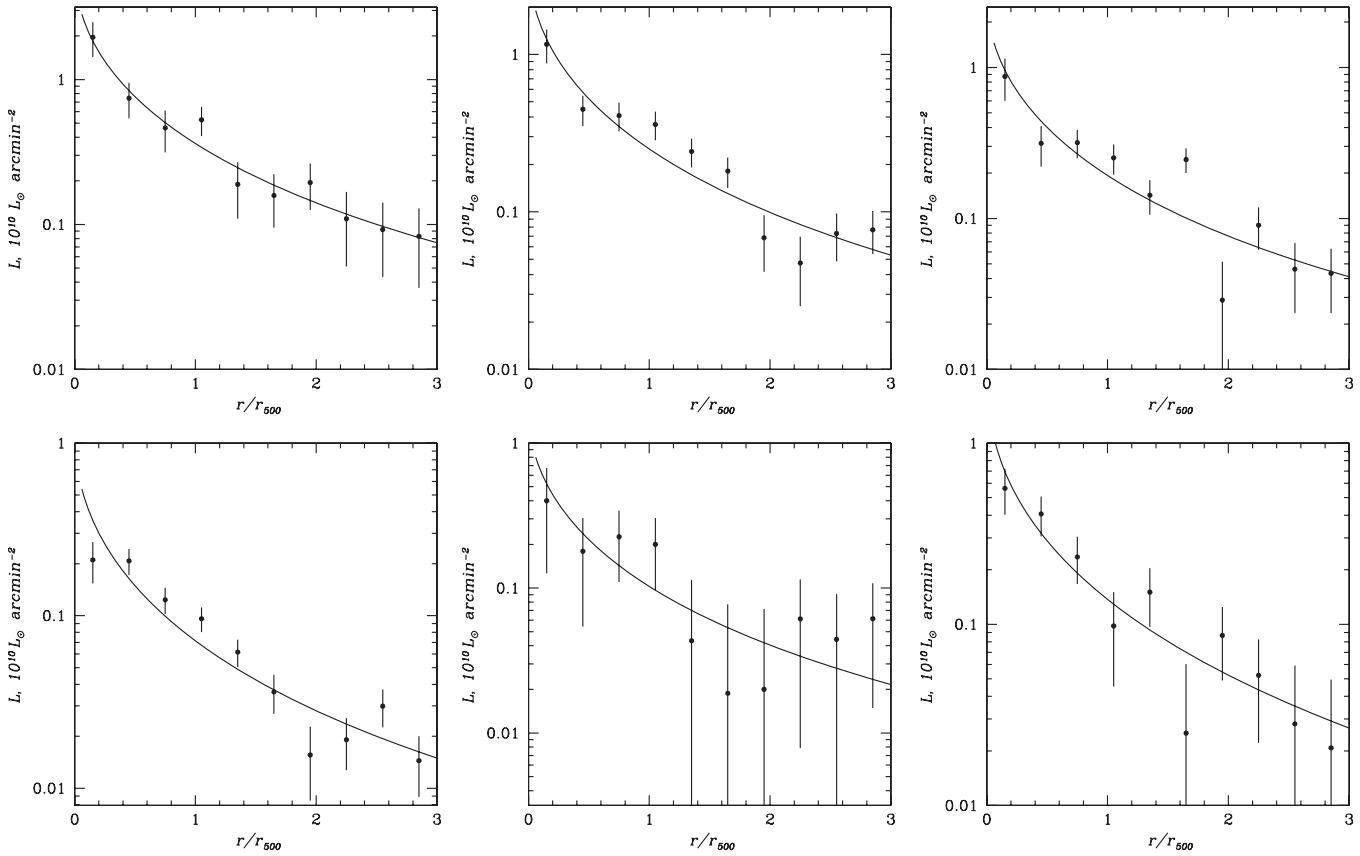

Figure 4. Background subtracted light profiles of FGs with SDSS data. Solid lines are a projected NFW profiles fits. Upper row from left to right: cl0259p0013, cl1038p4146, cl1042m0008. Bottom row from left to right: cl1159p5531, cl1340p4017, cl1416p2315.

5. Fit the light profile by a projected Navarro–Frenk–White function (Navarro et al. 1997) plus constant background. Fits for FGs with SDSS data are shown in Figure 4. A relative error in the bin is calculated as $(\sum_i \Delta L_i^2 / \sum_i L_i^2 + n_{\rm galaxies}^{-1})^{1/2}$, where ΔL_i is a luminosity error of the ith galaxy in the bin, L_i is a luminosity of the ith galaxy in the bin, $n_{\rm galaxies}$ is the number of galaxies in the bin, the sum is taken over all galaxies in the bin and the bin size is $0.3 r_{500}$.
6. In order to calculate the total cluster luminosity inside a given radius we integrate the NFW fit over the volume, then make corrections for the lost light (see step 3) and add the luminosity of cD galaxies. Our measurements are given in Table 3.

We show the $L_X - L_r (r < r_{500})$ correlation in Figure 5, where empty points correspond to FGs. We find that for a given optical luminosity, the FGs in our sample are not systematically brighter in the X-ray than other clusters. Indeed, four of the FGs reside on the upper envelope of the correlation, but there are also two FGs (cl1038p4146 and cl1159p5531) which appear X-ray faint compared to other clusters with similar optical luminosity.

We also compare our results with previous studies. K07 compared their FGs with other groups of galaxies studied by Helsdon & Ponman (2003) and Osmond & Ponman (2004). We show these data in Figure 6. We also add a compilation of optical luminosity measurements from Voevodkin et al. (2002), with optical luminosities rescaled to r_{500}. There appears to be general agreement in the trends between the FGs studied here and the FGs studied in K07; their distribution is also in agreement with

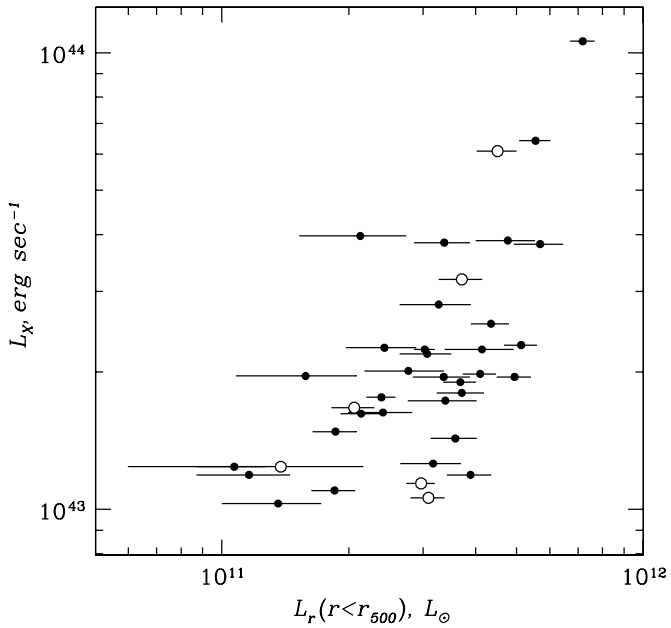

Figure 5. X-ray luminosity vs. optical luminosity measured inside r_{500}. Empty points show FGs.

the overall data for clusters, but not for groups. It is not clear whether the difference between FGs and other groups reported by K07 is real for less massive systems or if it is a result of systematic differences in analysis techniques used in different studies. We hope to address this issue in future work.

Table 3
Optical Luminosities of Clusters with SDSS Data

Name	z	L_X (10^{43} erg s^{-1})	r_{500} (kpc)	$L_r(r < r_{500})$ (10^{11} $L_\odot$)	M_{500} (10^{14} $M_\odot$)
cl0050m0929	0.199	3.81	784	5.69 ± 0.76	1.72
cl0223m0852	0.163	1.73	679	3.39 ± 0.63	1.07
cl0259p0013[fg]	0.194	3.19	757	3.71 ± 0.44	1.54
cl0304m0702	0.135	1.19	638	1.16 ± 0.29	0.86
cl0810p4216	0.064	2.24	754	3.03 ± 0.17	1.33
cl0838p1948	0.123	1.96	712	1.58 ± 0.50	1.19
cl0907p1639	0.076	1.98	731	4.10 ± 0.37	1.23
cl0910p6012*	0.181	1.24	627	1.07 ± 0.20	0.86
cl0943p1644	0.180	1.80	678	3.71 ± 0.48	1.09
cl1013p4933	0.133	1.95	707	3.36 ± 0.52	1.18
cl1038p4146[fg]	0.125	1.06	626	3.09 ± 0.29	0.81
cl1042m0008[fg]	0.138	1.67	683	2.06 ± 0.24	1.07
cl1124p4155	0.195	3.97	792	2.13 ± 0.60	1.76
cl1142p1008	0.119	1.63	687	2.41 ± 0.42	1.06
cl1142p1027	0.117	1.10	633	1.85 ± 0.22	0.83
cl1142p2145	0.131	1.95	708	4.95 ± 0.46	1.18
cl1146p2854	0.149	2.19	718	3.07 ± 0.43	1.25
cl1159p5531[fg]	0.081	1.14	650	2.97 ± 0.23	0.87
cl1212p2727	0.179	6.42	883	5.55 ± 0.47	2.40
cl1217p2255	0.140	1.48	665	1.86 ± 0.22	0.99
cl1222p2559	0.160	1.26	637	3.17 ± 0.52	0.88
cl1231p4137	0.176	2.26	712	2.43 ± 0.46	1.26
cl1235p4117	0.189	2.81	740	3.27 ± 0.63	1.43
cl1236p2550	0.175	2.01	696	2.77 ± 0.59	1.17
cl1340p3958	0.169	2.55	733	4.35 ± 0.45	1.36
cl1340p4017[fg]	0.171	1.24	631	1.38 ± 0.78	0.87
cl1341p2622	0.075	10.60	1030	7.18 ± 0.47	3.48
cl1349p4918	0.167	3.88	801	4.77 ± 0.77	1.77
cl1416p2315[fg]	0.138	6.09	893	4.51 ± 0.49	2.38
cl1436p5507	0.125	1.03	622	1.36 ± 0.36	0.80
cl1438p6423	0.146	1.43	659	3.58 ± 0.45	0.96
cl1515p4346	0.137	1.62	679	2.14 ± 0.23	1.05
cl1533p3108	0.067	1.90	728	3.68 ± 0.33	1.20
cl1537p1200	0.134	1.19	638	3.89 ± 0.47	0.87
cl1552p2013	0.136	2.29	730	5.13 ± 0.46	1.30
cl1629p2123	0.184	2.24	708	4.14 ± 0.76	1.25
cl1630p2434	0.066	1.76	717	2.39 ± 0.19	1.15
cl1639p5347	0.111	3.84	823	3.37 ± 0.51	1.82

Notes. [fg]Fossil group. *Due to a poor NFW fit, the luminosity is estimated in these cases as a sum of galaxy luminosities inside a given radius minus the sum of luminosities of background galaxies corrected for the area. Lost light corrections are also applied.

6. DISCUSSION

We have analyzed nearby ($z \leqslant 0.2$) and X-ray bright ($L_X \geqslant 10^{43}$ erg s^{-1}) clusters of galaxies from the 400d catalog. By evaluating known FGs against SDSS data, we have formulated slightly revised selection criteria for fossil systems. Our criteria are somewhat relaxed compared to those used by J03, but their advantage is that they select all previously known FGs (except for one system clearly misidentified as an FG).

Our main results can be summarized as follows:

1. We found seven new FGs in the 400d cluster survey. The images and descriptions of all 400d FGs are given in Appendix A.
2. We put new constraints on the number density of FGs. Our constraints are consistent with those obtained previously, but are tighter due to the larger number of FGs studied.
3. We measured optical luminosities of clusters with SDSS photometric data. Measurements of L_X–L_r correlations for these clusters show that FGs are similar to the overall cluster sample and follow the scaling relation of clusters of galaxies.

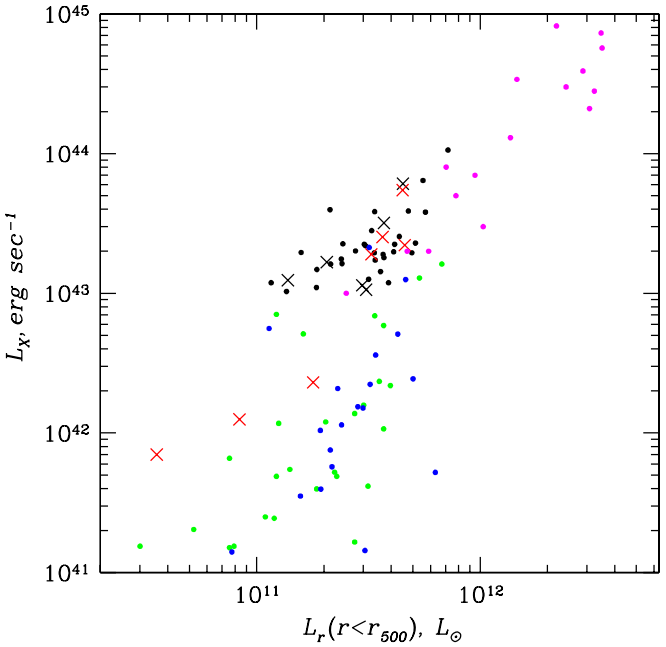

Figure 6. Comparison of our measurements with previous studies. Black dots and black crosses correspond to clusters and FGs from this work, red crosses show FGs from K07, blue and green dots represent groups studied in Helsdon & Ponman (2003) and Osmond & Ponman (2004) correspondingly. Magenta dots correspond to clusters of galaxies from Voevodkin et al. (2002).
(A color version of this figure is available in the online journal.)

Current definitions of FGs are not robust, i.e., the same object may be identified as an FG or not depending on what magnitude threshold and search radius is chosen. Due to the special variety of galaxy distributions in cluster potential wells, and due to cluster evolution, it is hard to motivate a strict definition of FGs using simple observables. Moreover, there is another major obstacle from the observational perspective for FG searches—the group membership, which cannot be firmly established observationally. While precise redshift measurements can weed out most of the projected galaxies, they are not enough to establish the presence or absence of a gravitational bond between a given galaxy and the group, nor can they provide a measurement of the distance from a given galaxy to the center along the line of sight. It is evident that the situation is much more complicated if precise redshift measurements are not available. The absence of such redshift measurements may account for the differences in the number density of FGs found in observations and in simulations (see e.g., Dariush et al. 2007).

We have found that massive FGs are not too much different from clusters of galaxies in the L_X–$L_{\rm opt}$ plane. This result is in contradiction with the findings of J03 and K07 who state that for a given optical luminosity FGs are more X-ray luminous. Here, we point out that it is more correct to say that for a given X-ray luminosity FGs are less luminous in the optical band than normal groups. This can be shown from the following argument: groups and clusters of galaxies are primarily characterized by their total mass. FGs are not different from groups and clusters of galaxies in the L_X–T and $M_{\rm tot}$–T planes (K07; Sun et al. 2008). Therefore for the given total mass, FGs have the same

L_X as normal groups, and therefore for the given L_X FGs have lower L_{opt} than normal groups.[8]

Our result shows that during their evolution both clusters and FGs have formed almost the same amount of stars. The only difference between FGs and clusters is the Δm_{12} gap between the brightest and second-brightest galaxy. For a given object, the classification for being a FG or a normal group(cluster) depends on the value chosen for the Δm_{12} gap and on the radius within we are searching for the second brightest galaxy. There are clusters in our sample which are not FGs only because one galaxy inside the search radius does not strictly satisfy the Δm_{12} criterion.

Obviously, for a given L_X the optical luminosity of clusters with e.g., $\Delta m_{12} = 1.6$ will not be significantly larger than the optical luminosity of clusters with $\Delta m_{12} = 1.7$. On the other hand, if we find a FG which has a bright galaxy just outside the search radius, this bright galaxy will increase the optical luminosity of this FG and make it basically equal to the optical luminosity of clusters which have one or two bright galaxies within the search radius. While the two systems described are rather similar with respect to L_X and optical luminosity, we would classify one as normal cluster and the other as FG. It is therefore not surprising that we do not see much difference between clusters and FGs in Figure 5—there is not sharp separation between the two populations. In addition, FGs do not show any other unexpected features, e.g., concentration (Sun et al. 2008; von Benda-Beckmann et al. 2008) or boxiness–diskiness (Diaz-Gimenez et al. 2008) are similar in their distribution for FGs and for other systems. Taking all these results together, this leads currently to the conclusion, that FGs might in fact not be a peculiar class of objects. Such a conclusion is also in agreement with recent simulation results, e.g., von Benda-Beckmann et al. (2008) and Diaz-Gimenez et al. (2008).

Our results might hint to some clues about the formation history of FGs. There are seed places for cluster formation, where the central galaxy was formed early on by mergers of several bright galaxies located close to each other. Such galaxy mergers can effectively take place at high redshifts as was shown in many simulations (see, e.g., Barnes 1989). The magnitude gap Δm_{12} inside a given radius is formed in the following way: all bright galaxies merged to form the central bright galaxy. Other (not merged) bright cluster galaxies have either orbits such that the infall time is larger than the Hubble time or just have not entered the search radius at the moment of observation. This scenario explains the existence of clusters in our sample which are not FGs due to the presence of only one bright galaxy inside the search radius not satisfying the Δm_{12} criterion. Such a galaxy could enter the central cluster part and made it a non-FG. Cases like this are also seen in simulations (von Benda-Beckmann et al. 2008).

In conclusion, in order to gain a better understanding of the nature of FGs it is important to have a more reliable FG definition than available at present.

This work was supported by the LDRD program at Los Alamos National Laboratory. Data from SDSS DR6 were used extensively in this study. The SDSS is managed by the Astrophysical Research Consortium for the Participating Institutions. The Participating Institutions are the American Museum of Natural History, Astrophysical Institute Potsdam, University of Basel, University of Cambridge, Case Western Reserve University, University of Chicago, Drexel University, Fermilab, the Institute for Advanced Study, the Japan Participation Group, Johns Hopkins University, the Joint Institute for Nuclear Astrophysics, the Kavli Institute for Particle Astrophysics and Cosmology, the Korean Scientist Group, the Chinese Academy of Sciences (LAMOST), Los Alamos National Laboratory, the Max-Planck-Institute for Astronomy (MPIA), the Max-Planck-Institute for Astrophysics (MPA), New Mexico State University, Ohio State University, University of Pittsburgh, University of Portsmouth, Princeton University, the United States Naval Observatory, and the University of Washington. We acknowledge useful discussions regarding SDSS photometry with Chris Miller and Adrian Pope. This research has made use of the NASA/IPAC Extragalactic Database (NED) which is operated by the Jet Propulsion Laboratory, California Institute of Technology, under contract with the National Aeronautics and Space Administration.

APPENDIX

DESCRIPTION OF THE FOSSIL GROUPS

In this Appendix, we provide a detailed description of all 12 FGs studied in this paper. This information will be useful for future FG studies. For example, higher quality data for the systems studied here might become available or one might want to refine the definition of FGs further. In either case, detailed information available regarding these FGs will be helpful.

In all images the inner black circle marks the radius $0.7r_{500}$, which we have adopted as our search radius. The outer black circle shows the radius r_{500}, and a white cross marks the X-ray center. The white arrow inside $0.7r_{500}$ points to the second brightest galaxy in the group. The second white arrow inside the ring $0.7r_{500}$—r_{500} (if present) shows the second brightest galaxy within the increased search radius. Black arrows show projected galaxies with known spectroscopic redshifts, which do not belong to the FG. Such galaxies could have led to an incorrect classification of the groups as being non-fossil, if the redshift measurements were not available.

cl0245p0936

cl0245p0936 is one of the new fossil systems found by us in the 400d survey at $z = 0.147$. The RTT150 CCD unfortunately does not cover a full circle with radius $0.7r_{500}$. The coverage is shown as a white square in Figure 7. The second brightest galaxy is marked by the white arrow, $\Delta m_{12} = 2.15$. A visual inspection of the DSS2 image reveals that inside $0.7r_{500}$ there are no galaxies brighter than the second brightest. However, within r_{500} there may be galaxies which are brighter than the second brightest. It is not possible to conclude from the currently available data whether those galaxies belong to the system or not.

cl0259p0013

cl0259p0013 is another new fossil system discovered by us at $z = 0.194$. For this object, optical data from the SDSS are available. The second brightest galaxy is marked with a white arrow in Figure 7 with $\Delta m_{12} = 2.25$. If we increase the search radius up to r_{500} the second brightest galaxy will be at R.A. = $02^h59^m31\overset{s}{.}704$, decl. = $+00^\circ17^m21\overset{s}{.}38$ (another white arrow) for

[8] J03 have mentioned such a possibility but their data set then would have indicated that FGs have an abnormally high mass-to-light ratio. More recent results by K07 show that the M/L ratios for FGs are comparable with those found for clusters and groups (see their Figure 10).

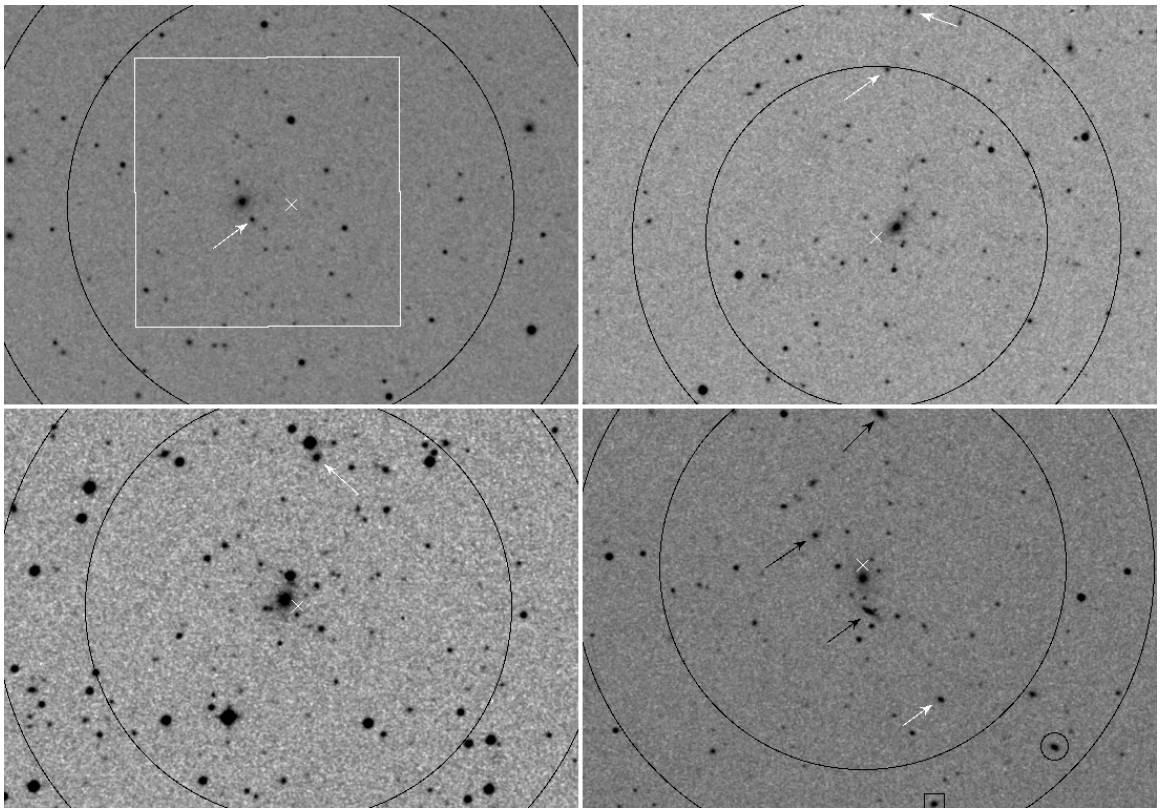

Figure 7. DSS2 images of FGs. From left to right, top to bottom: cl0245p0936, cl0259p0013, cl0532m4614, and cl1038p4146.

which $m_{12} = 1.92$, i.e., this group would satisfy our magnitude threshold, even with the increased search radius.

cl0532m4614

cl0532m4614 is the third newly identified fossil system. The object is at $z = 0.135$. The optical image was obtained on the LCO-40 telescope. The second brightest galaxy is shown by a white arrow in Figure 7 with $\Delta m_{12} = 1.90$. If we increase the search radius up to r_{500} we do not find any galaxy brighter than the second brightest galaxy and therefore the object would be a fossil group even with a larger search radius.

cl1038p4146

cl1038p4146 is the fourth of our new fossil systems. For this object, which is at $z = 0.125$, SDSS data are available. The second brightest galaxy, for which the redshift is known, is marked by a white arrow in Figure 7 with $\Delta m_{12} = 1.87$. The image shows three bright projected galaxies (black arrows in Figure 7) for which redshifts are fortunately available. Without these redshifts, the object would not have been classified as an FG. Increasing the search radius up to r_{500} reveals two bright galaxies belonging to the cluster, which would not allow us to classify the system as an FG. These galaxies have coordinates $10^{\rm h}37^{\rm m}44\overset{\rm s}{.}679 + 41^\circ43^{\rm m}49\overset{\rm s}{.}89$, $\Delta m_{12} = 1.12$ (small black circle in Figure 7) and $10^{\rm h}37^{\rm m}54\overset{\rm s}{.}881 + 41^\circ42^{\rm m}49\overset{\rm s}{.}86$, $\Delta m_{13} = 1.41$ (small black box in Figure 7).

cl1042m0008

cl1042m0008 is another newly discovered fossil system. SDSS data are available for this object, which is at $z = 0.138$. The second brightest galaxy is shown by a white arrow in Figure 8 with $\Delta m_{12} = 1.80$. Increasing the search radius up to r_{500} does not change its FG identification (the second brightest galaxy remains the same). More bright galaxies appear, but they are all projected according to their spectroscopic redshifts. Their positions are indicated by black arrows in Figure 8.

cl1110m2957

cl1110m2957 is the sixth new FG. For this object, which is at $z = 0.20$, data from the Danish 1.54 m telescope is available. The second brightest galaxy is marked by a white arrow (see Figure 8) with $\Delta m_{12} = 1.78$. With an increase of the search radius to r_{500}, the object would no longer be classified as an FG. The new bright galaxy is located at R.A. $= 11^{\rm h}10^{\rm m}10\overset{\rm s}{.}667$, decl. $= -29^\circ54^{\rm m}08\overset{\rm s}{.}92$, with $m_{12} = 1.32$, and is shown by another white arrow in Figure 8. The redshifts for both second brightest galaxies are unknown.

cl1159p5531

cl1159p5531 has been previously identified as an OLEG Vikhlinin et al. (1999) using X-ray data from *ROSAT* PSPC pointed observation and optical data from the FLWO2 telescope (the size of CCD image is shown by the white rectangle in Figure 8). This object has SDSS data and we also used it as a reference to re-define the FG criteria. The second brightest galaxy inside $0.7r_{500}$ with $\Delta m_{12} = 2.73$ has a measured spectroscopic redshift and belongs to the cluster (see white arrow in Figure 8), which is at $z = 0.081$. If we increase the search radius, this group may still be considered an FG (another bright galaxy has $\Delta m_{12} = 1.69$, it belongs to the group, see the white arrow in Figure 8, and see also the first panel in Figure 1), even though Δm_{12} would be slightly smaller than our threshold.

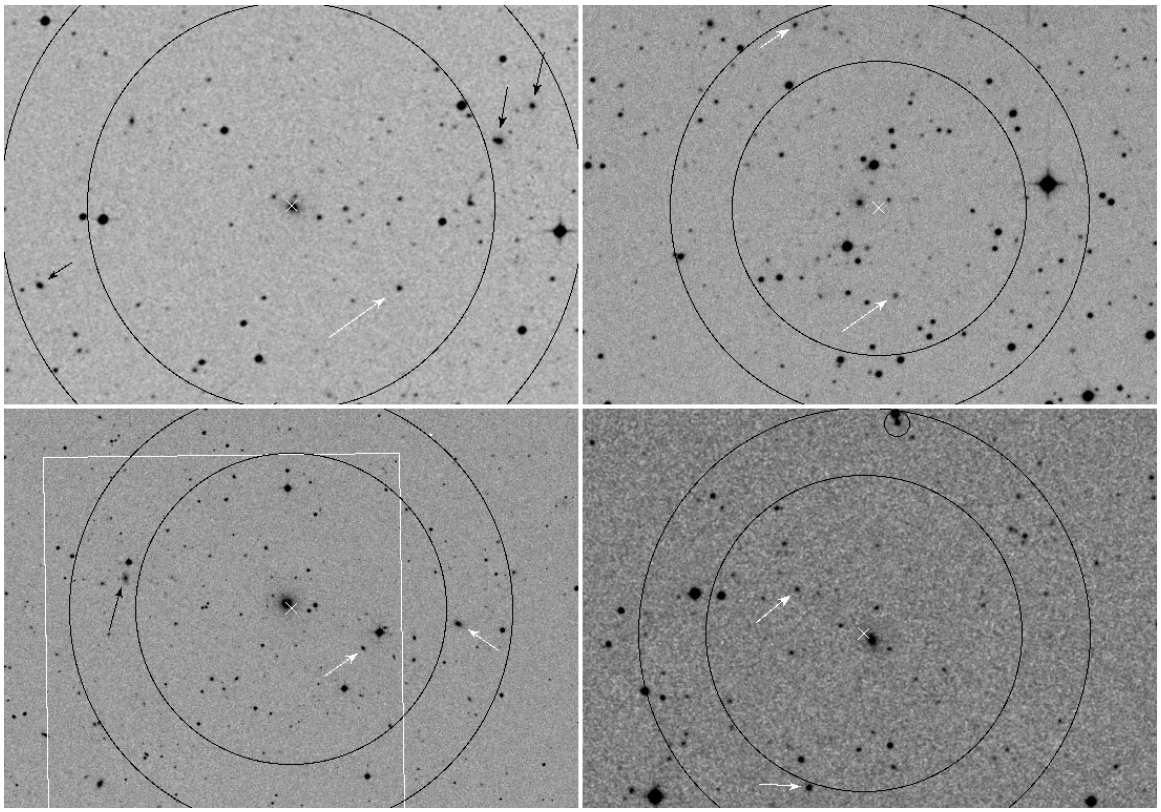

Figure 8. DSS2 images of FGs. From left to right and top to bottom: cl1042m0008, cl1110m2957, cl1159p5531, and cl1340p4017.

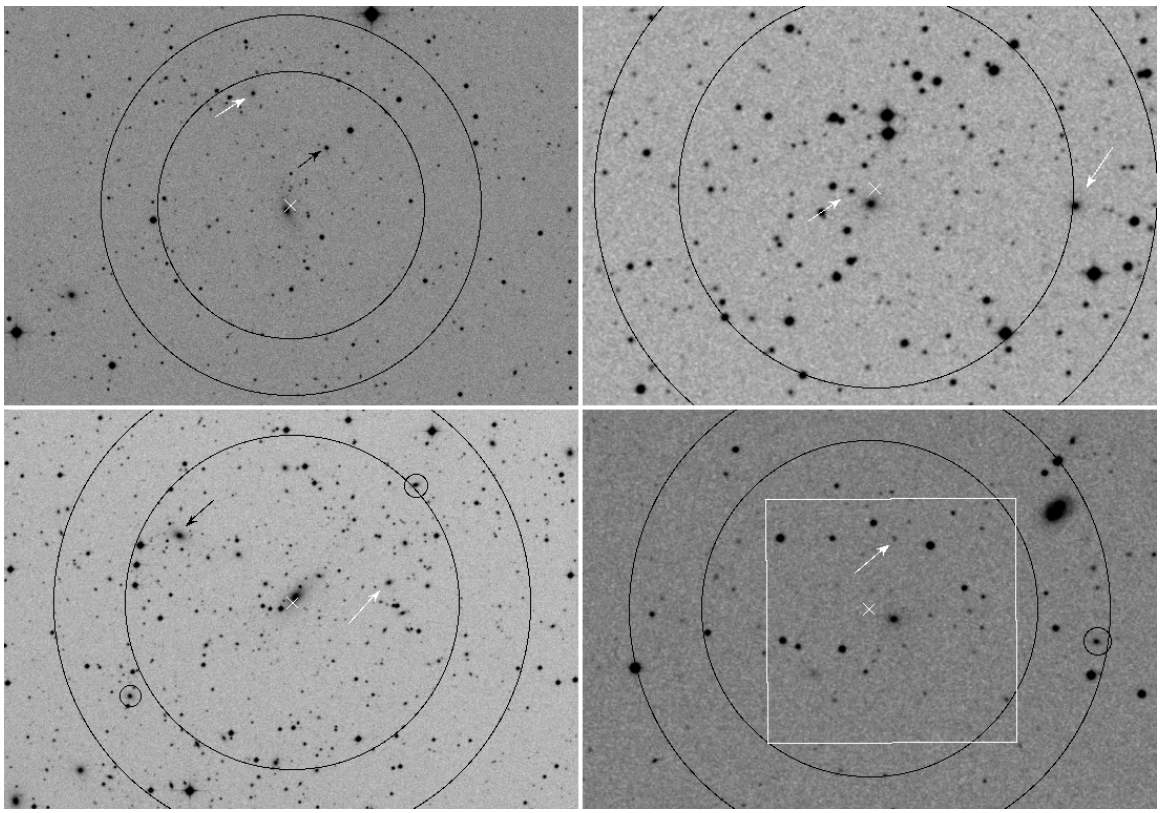

Figure 9. DSS2 images of FGs. From left to right and top to bottom: cl1416p2315, cl2114m6800, cl2220m5228, and cl2247p0337.

cl1340p4017

cl1340p4017 is the very first identified fossil group (Ponman et al. 1994). SDSS data is now available for this object, which is at $z = 0.171$, and we used it to re-define the FG criteria (see second panel in Figure 1). The second brightest galaxy inside a search radius $0.7r_{500}$ is shown by a white arrow and has $\Delta m_{12} = 2.47$. Increasing the search radius to r_{500}

reveals two more bright galaxies (see the white arrow inside the ring in Figure 8 for a galaxy with known spectroscopic redshift and $\Delta m_{12} = 1.31$, and a black circle for a galaxy with only photometric data and $\Delta m_{12} = 1.58$). With these galaxies included, this object would not be classified as an FG.

cl1416p2315

cl1416p2315 is the first fossil cluster to be discovered. It was studied by different research groups (J03; Cypriano et al. 2006; Khosroshahi et al. 2006). Since SDSS data are available for this object, which is at $z = 0.138$, we also used it as a reference for deciding our FG criteria. The second brightest galaxy is marked by a white arrow in Figure 9 with $\Delta m_{12} = 1.7$. The black arrow points to a galaxy which according to Cypriano et al. (2006) does not belong to the cluster.[9] Increasing the search radius to r_{500} does not reveal any more bright galaxies, which might have changed the classification of the system as an FG (see also the third panel of Figure 1).

cl2114m6800

cl2114m6800 was originally identified as an OLEG Vikhlinin et al. (1999). The system, which is at $z = 0.130$, satisfies our FG criteria as well. The second brightest galaxy is marked by a white arrow (see Figure 9) with $\Delta m_{12} = 1.99$. If we increase the search radius to r_{500}, we find another bright galaxy 2MASX J21134604 − 6801297, which does not obey $\Delta m_{12} \geqslant 1.7$. Since the redshift of this galaxy is unknown, it is not clear that it belongs to the group.

cl2220m5228

cl2220m5228 is the seventh new FG discovered. For this object we do not have a CCD image, but only a DSS2 image. However, we have found ENACS data with photometry obtained in the *R* filter and measured redshifts for the central and several other bright galaxies. The group is at $z = 0.102$. In Figure 9, the second brightest galaxy is marked by a white arrow with $\Delta m_{12} = 2.21$. The black arrows point to foreground galaxies. If the search radius would be increased to r_{500} two more bright galaxies (black circles) would have to be considered which would make this group a normal group. Since we do not have redshift information for these galaxies it is unclear if they in fact belong to the system.

cl2247p0337

cl2247p0337 is another previously discovered OLEG (Vikhlinin et al. 1999). It would also pass our criteria for a fossil system. However, the CCD image from RTT150 does not completely cover the search region (see the white rectangle in Figure 9).

The examination of the larger DSS2 image shows that there is no other bright galaxy inside the search radius. Therefore, we consider this object to be an FG (the second brightest galaxy with $\Delta m_{12} = 2.56$ is marked by the white arrow). If we increase the search radius up to r_{500}, we find a big foreground galaxy NGC 7376. A visual comparison of angular sizes of this galaxy and the central cluster galaxy leads to the conclusion that it must be foreground. Another bright galaxy, which could make this object a normal group, is marked by a black circle in Figure 9. Since neither photometry nor redshift of this galaxy are known, we cannot determine if it belongs to the group or not.

[9] Actually, there are two galaxies (see SDSS DR6 data, or Cypriano et al. 2006). We are referring to the galaxy with coordinates: $14^h16^m21\overset{s}{.}745 + 23°17^m20\overset{s}{.}97$. The second galaxy is significantly dimmer.

REFERENCES

Abazajian, K. N., et al. 2009, ApJS, 182, 543
Adelman-McCarthy, J. K., et al. 2008, ApJS, 175, 297
Barnes, J. E. 1989, Nature, 338, 123
Bertin, E., & Arnouts, S. 1996, A&AS, 117, 393
Blanton, M. R., & Roweis, S. 2007, AJ, 133, 734
Burenin, R. A., Vikhlinin, A., Hornstrup, A., Ebeling, H., Quintana, H., & Mescheryakov, A. 2007, ApJS, 172, 561
Cash, W. 1979, ApJ, 228, 939
Cypriano, E. S., Mendes de Oliveira, C. L., & Sodré, L. J. 2006, AJ, 132, 514
Dariush, A., Khosroshahi, H. G., Ponman, T. J., Pearce, F., Raychaudhury, S., & Hartley, W. 2007, MNRAS, 382, 433
Diaz-Gimenez, E., Ragone-Figueroa, C., Muriel, H., & Mamon, G. 2008, A&A, 490, 965
D'Onghia, E., Sommer-Larsen, J., Romeo, A. D., Burkert, A., Pedersen, K., Portinari, L., & Rasmussen, J. 2005, ApJ, 630, L109
Fukugita, M., Ichikawa, T., Gunn, J. E., Doi, M., Shimasaku, K., & Schneider, D. P. 1996, AJ, 111, 1748
Jones, L. R., Ponman, T. J., Horton, A., Babul, A., Ebeling, H., & Burke, D. J. 2003, MNRAS, 343, 627
Helsdon, S. F., & Ponman, T. J. 2003, MNRAS, 340, 485
Katgert, P., Mazure, A., den Hartog, R., Adami, C., Biviano, A., & Perea, J. 1998, A&AS, 129, 399
Khosroshahi, H. G., Maughan, B. J., Ponman, T. J., & Jones, L. R. 2006, MNRAS, 369, 1211
Khosroshahi, H. G., Ponman, T. J., & Jones, L. R. 2006, MNRAS, 372, L68
Khosroshahi, H. G., Ponman, T. J., & Jones, L. R. 2007, MNRAS, 377, 595
La Barbera, F., de Carvalho, R. R., de la Rosa, I. G., Sorrentino, G., Gal, R. R., & Kohl-Moreira, J. L. 2009, AJ, 137, 3942
Mendes de Oliveira, C. L., Cypriano, E. S., & Sodré, L. J. 2006, AJ, 131, 158
Milosavljević, M., Miller, C. J., Furlanetto, S. R., & Cooray, A. 2006, ApJ, 637, L9
Mulchaey, J. S., & Zabludoff, A. I. 1999, ApJ, 514, 133
Navarro, J. F., Frenk, C. S., & White, S. D. M. 1997, ApJ, 490, 493
Osmond, J. P. F., & Ponman, T. J. 2004, MNRAS, 350, 1511
O'Sullivan, E., Forbes, D. A., & Ponman, T. J. 2001, MNRAS, 328, 461
Oyaizu, H., Lima, M., Cunha, C. E., Lin, H., Frieman, J., & Sheldon, E. S. 2008, ApJ, 674, 768
Ponman, T. J., Allan, D. J., Jones, L. R., Merrifield, M., McHardy, I. M., Lehto, H. J., & Luppino, G. A. 1994, Nature, 369, 462
Press, W. H., & Schechter, P. 1974, ApJ, 187, 425
Romer, A. K., et al. 2000, ApJS, 126, 209
Santos, W. A., Mendes de Oliveira, C., & Sodré, L. J. 2007, AJ, 134, 1551
Schechter, P. 1976, ApJ, 203, 297
Schlegel, D. J., Finkbeiner, D. P., & Davis, M. 1998, ApJ, 500, 525
Sun, M., Voit, G. M., Donahue, M., Jones, C., Forman, W., & Vikhlinin, A. 2009, ApJ, 693, 1142
Vikhlinin, A., McNamara, B. R., Hornstrup, A., Quintana, H., Forman, W., Jones, C., & Way, M. 1999, ApJ, 520, L1
Vikhlinin, A., McNamara, B. R., Forman, W., Jones, C., Quintana, H., & Hornstrup, A. 1998, ApJ, 502, 558
Vikhlinin, A., et al. 2008, arXiv:0805.2207
Voevodkin, A. A., Vikhlinin, A. A., & Pavlinsky, M. N. 2002, Astron. Lett., 28, 366
von Benda-Beckmann, A. M., D'Onghia, E., Gottlöber, S., Hoeft, M., Khalatyan, A., Klypin, A., & Müller, V. 2008, MNRAS, 386, 2345
Yoshioka, T., Furuzawa, A., Takahashi, S., Tawara, Y., Sato, S., Yamashita, K., & Kumai, Y. 2004, Adv. Space Res., 34, 2525
Zibetti, S., Pierini, D., & Pratt, G. W. 2009, MNRAS, 392, 525